J|A|C|S ARTICLES

Published on Web 03/17/2010

Reversible Phase Transitions in Self-Assembled Monolayers at the Liquid−Solid Interface: Temperature-Controlled Opening and Closing of Nanopores

Rico Gutzler,*,† Thomas Sirtl,† Jürgen F. Dienstmaier,† Kingsuk Mahata,‡ Wolfgang M. Heckl,# Michael Schmittel,‡ and Markus Lackinger*,†

Department of Earth and Environmental Sciences and Center for NanoScience (CeNS), Ludwig-Maximilians-University, Theresienstrasse 41, 80333 Munich, Germany, Center of Micro and Nanochemistry and Engineering, Organische Chemie I, University Siegen, Adolf-Reichwein-Strasse 2, 57068 Siegen, Germany, Deutsches Museum, Museumsinsel 1, 80538 Munich, Germany, and Department of Physics, TUM School of Education, Technical University Munich, Schellingstrasse 33, 80333 Munich, Germany

Received October 19, 2009; E-mail: rico.gutzler@lrz.uni-muenchen.de; markus@lackinger.org

Abstract: We present a variable-temperature study of monolayer self-assembly at the liquid−solid interface. By means of *in situ* scanning tunneling microscopy (STM), reversible phase transitions from a nanoporous low-temperature phase to a more densely packed high-temperature phase are observed. The occurrence of the phase transition and the respective transition temperature were found to depend on the type of solvent and solute concentration. Estimates of the entropic cost and enthalpic gain upon monolayer self-assembly suggest that coadsorption of solvent molecules within the cavities of the nanoporous structure renders this polymorph thermodynamically stable at low temperatures. At elevated temperatures, however, desorption of these relatively weakly bound solvent molecules destabilizes the nanoporous polymorph, and the densely packed polymorph becomes thermodynamically favored. Interestingly, the structural phase transition provides external control over the monolayer morphology and, for the system under discussion, results in an effective opening and closing of supramolecular nanopores in a two-dimensional molecular monolayer.

Introduction

Self-assembly of ordered monolayers at the liquid−solid interface has been proven to be well suited for functionalizing surfaces and, thus, has become a topic of elaborate research.[1−5] Especially porous networks, which can be utilized as supramolecular host systems for defined coadsorption of nanoscopic guests, have received broad interest.[6−11]Tailoring morphology, size, and functionalization of porous networks thus remains a topic of fundamental interest in nanotechnology. The monolayer morphology is primarily governed by the structure and functional groups of the molecule,[12−14] but can also depend on the type of solvent,[15−18] concentration,[5,19−21] substrate,[22] substrate-mediated interactions,[23] and other factors. Among all important parameters for self-assembly at the liquid−solid interface, temperature is probably the one least studied, and only a few examples are reported in the literature.[21,24−30] For instance, English and Hipps use STM to reveal the progressive desorption of coronene from Au(111) between room temperature and 55 °C (*in situ*, up to 105 °C *ex-situ*).[27] However, in many variable-temperature studies samples are just conditioned at elevated temperatures, while measurements are still conducted at room temperature.

Although temperature is a vital parameter for any self-assembly because it directly affects both thermodynamics and kinetics, little is known about its influence on physisorbed

† Ludwig-Maximilians-University.
‡ University Siegen.
# Deutsches Museum and Technical University Munich.

(1) Barth, J. V.; Costantini, G.; Kern, K. *Nature* **2005**, *437* (7059), 671–679.
(2) De Feyter, S.; De Schryver, F. C. *J. Phys. Chem. B* **2005**, *109* (10), 4290–4302.
(3) Elemans, J. A. A. W.; De Feyter, S. *Soft Matter* **2009**, *5* (4), 721–735.
(4) Kühnle, A. *Curr. Opin. Colloid Interface Sci.* **2009**, *14* (2), 157–168.
(5) Yang, Y. L.; Wang, C. *Curr. Opin. Colloid Interface Sci.* **2009**, *14* (2), 135–147.
(6) Kudernac, T.; Lei, S. B.; Elemans, J. A. A. W.; De Feyter, S. *Chem. Soc. Rev.* **2009**, *38* (2), 402–421.
(7) Madueno, R.; Raisanen, M. T.; Silien, C.; Buck, M. *Nature* **2008**, *454* (7204), 618–621.
(8) Theobald, J. A.; Oxtoby, N. S.; Phillips, M. A.; Champness, N. R.; Beton, P. H. *Nature* **2003**, *424* (6952), 1029–1031.
(9) Stepanow, S.; Lingenfelder, M.; Dmitriev, A.; Spillmann, H.; Delvigne, E.; Lin, N.; Deng, X. B.; Cai, C. Z.; Barth, J. V.; Kern, K. *Nat. Mater.* **2004**, *3* (4), 229–233.
(10) Griessl, S. J. H.; Lackinger, M.; Jamitzky, F.; Markert, T.; Hietschold, M.; Heckl, W. M. *Langmuir* **2004**, *20* (21), 9403–9407.
(11) Kühne, D.; Klappenberger, F.; Decker, R.; Schlickum, U.; Brune, H.; Klyatskaya, S.; Ruben, M.; Barth, J. V. *J. Am. Chem. Soc.* **2009**, *131* (11), 3881–3883.
(12) Tahara, K.; Furukawa, S.; Uji-I, H.; Uchino, T.; Ichikawa, T.; Zhang, J.; Mamdouh, W.; Sonoda, M.; De Schryver, F. C.; De Feyter, S.; Tobe, Y. *J. Am. Chem. Soc.* **2006**, *128* (51), 16613–16625.
(13) Kampschulte, L.; Werblowsky, T. L.; Kishore, R. S. K.; Schmittel, M.; Heckl, W. M.; Lackinger, M. *J. Am. Chem. Soc.* **2008**, *130* (26), 8502–8507.
(14) Gutzler, R.; Lappe, S.; Mahata, K.; Schmittel, M.; Heckl, W. M.; Lackinger, M. *Chem. Commun.* **2009**, (6), 680–682.

 10.1021/ja908919r

monolayers at the liquid−solid interface. For 1,3,5-tris(4-carboxyphenyl)benzene (BTB, cf. Figure 1a) monolayers, temperature-dependent structural phase transitions were observed under vacuum conditions on the Ag(111) surface.[31] Yet, most likely driven by a stepwise deprotonation of the carboxylic groups, these phase transitions are not reversible.

Herein we demonstrate how the morphology of BTB monolayers at the carboxylic acid/graphite interface specifically can be switched bidirectionally by lowering and raising the temperature. As detailed below, interfacial BTB monolayers show a fully reversible temperature-driven structural phase transition, changing from an open pore network to a nonporous, densely packed structure. Accordingly, nanopores can be closed at slightly elevated temperatures and opened again by cooling the sample below the transition temperature. Such a reversible process opens venues for various applications in which guest coadsorption is controlled by temperature, as a densely packed structure in contrast to an open-pore structure does not facilitate coadsorption of molecular guests.

Our experimental findings can be explained and are rationalized by thermodynamic considerations, where the free energies of adsorption of both polymorphs are evaluated from a molecule-based estimation of enthalpic gains and entropic costs.

Results and Discussion

Solvent Dependence. Three different carboxylic acids served as solvents, namely heptanoic (**7A**), octanoic (**8A**), and nonanoic acid (**9A**). At room temperature with **7A** as solvent, BTB furnishes a previously unobserved densely packed row structure on HOPG with striped appearance (Figure 1b). In **8A**, the row structure is found in coexistence with the chicken-wire structure, a hexagonal, less dense open-pore network (Figure 1c) that is quite common for other 3-fold symmetric tricarboxylic acids as well.[14,32] At room temperature, **9A** as solvent exclusively yields the chicken-wire structure (Figure 1d). Models of the respective polymorphs are presented in Figure 1e,f.

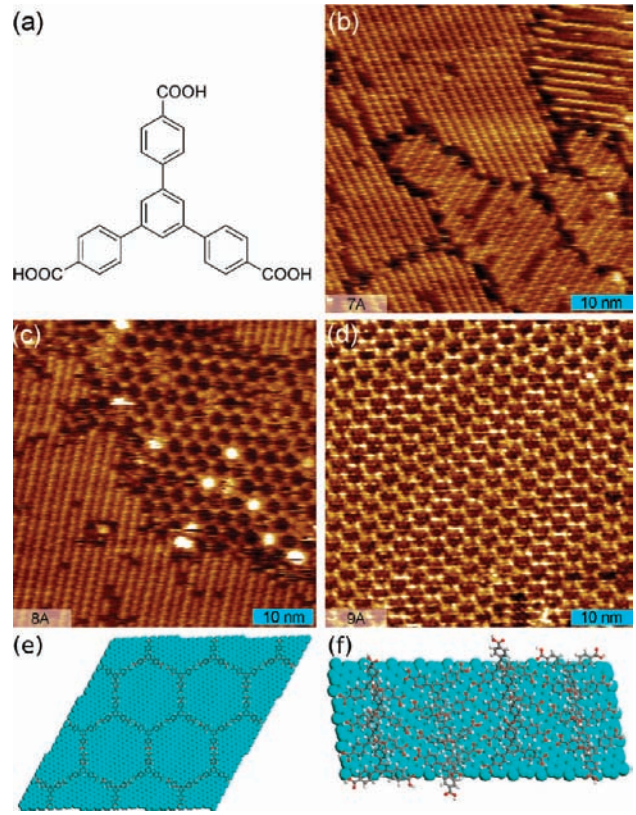

Figure 1. (a) Chemical structure of 1,3,5-tris(4-carboxyphenyl)benzene (BTB). STM topographs of BTB monolayers at the (b) heptanoic acid/graphite (V_{bias} = 0.80 V, I_T = 77 pA), (c) octanoic acid/graphite (V_{bias} = 1.10 V, I_T = 92 pA), and (d) nonanoic acid/graphite interface (V_{bias} = 1.15 V, I_T = 71 pA). In all cases saturated solutions were used and topographs were recorded at room temperature. (e) Ball-and-stick model of a chicken-wire BTB monolayer on graphite; nine unit cells are depicted (cyan: graphite substrate, gray: carbon, white: hydrogen, red: oxygen). (f) Top view of a ball-and-stick model of the row structure of BTB on graphite; eight unit cells are depicted. Adjacent rows are interconnected via hydrogen bonds.

Temperature Dependence. A home-built heatable sample stage facilitates STM measurements at the liquid−solid interface from room temperature up to ∼70 °C. Heating the BTB/**7A** system to over 60 °C did not result in any change of the monolayer morphology. At all intermediate temperatures, exclusively the row structure was observed. In **8A**, the coexistence of both phases prevailed up to ∼43 °C. Above this temperature the sample was entirely covered with the row structure. Similarly, in **9A** the chicken-wire structure was stable up to ∼55 °C, while at temperatures above only the row structure could be observed. In order to verify the reversibility of the BTB phase transition, several heat−cool cycles were conducted in **8A** and **9A**, where images were repeatedly acquired below as well as above the respective transition temperature

(15) Kampschulte, L.; Lackinger, M.; Maier, A. K.; Kishore, R. S. K.; Griessl, S.; Schmittel, M.; Heckl, W. M. *J. Phys. Chem. B* **2006**, *110* (22), 10829–10836.
(16) Mamdouh, W.; Uji-i, H.; Ladislaw, J. S.; Dulcey, A. E.; Percec, V.; De Schryver, F. C.; De Feyter, S. *J. Am. Chem. Soc.* **2006**, *128* (1), 317–325.
(17) Li, Y. B.; Ma, Z.; Qi, G. C.; Yang, Y. L.; Zeng, Q. D.; Fan, X. L.; Wang, C.; Huang, W. *J. Phys. Chem. C* **2008**, *112* (23), 8649–8653.
(18) Zhang, X.; Chen, Q.; Deng, G. J.; Fan, Q. H.; Wan, L. J. *J. Phys. Chem. C* **2009**, *113* (36), 16193–16198.
(19) Lei, S. B.; Tahara, K.; De Schryver, F. C.; Van der Auweraer, M.; Tobe, Y.; De Feyter, S. *Angew. Chem., Int. Ed.* **2008**, *47* (16), 2964–2968.
(20) So, C. R.; Tamerler, C.; Sarikaya, M. *Angew. Chem., Int. Ed.* **2009**, *48* (28), 5174–5177.
(21) Palma, C. A.; Bjork, J.; Bonini, M.; Dyer, M. S.; Llanes-Pallas, A.; Bonifazi, D.; Persson, M.; Samorì, P. *J. Am. Chem. Soc.* **2009**, *131*, 13062–13071.
(22) Klappenberger, F.; Cañas-Ventura, M. E.; Clair, S.; Pons, S.; Schlickum, U.; Qu, Z. R.; Strunskus, T.; Comisso, A.; Wöll, C.; Brune, H.; Kern, K.; De Vita, A.; Ruben, M.; Barth, J. V. *ChemPhysChem* **2008**, *9* (17), 2522–2530.
(23) Wang, Y. F.; Ge, X.; Manzano, C.; Korger, J.; Berndt, R.; Hofer, W. A.; Tang, H.; Cerda, J. *J. Am. Chem. Soc.* **2009**, *131* (30), 10400–10402.
(24) Valiokas, R.; Ostblom, M.; Svedhem, S.; Svensson, S. C. T.; Liedberg, B. *J. Phys. Chem. B* **2000**, *104* (32), 7565–7569.
(25) Azzam, W.; Bashir, A.; Terfort, A.; Strunskus, T.; Wöll, C. *Langmuir* **2006**, *22* (8), 3647–3655.
(26) Bleger, D.; Kreher, D.; Mathevet, F.; Attias, A. J.; Schull, G.; Huard, A.; Douillard, L.; Fiorini-Debuischert, C.; Charra, F. *Angew. Chem., Int. Ed.* **2007**, *46* (39), 7404–7407.
(27) English, W. A.; Hipps, K. W. *J. Phys. Chem. C* **2008**, *112* (6), 2026–2031.
(28) Kong, X. H.; Deng, K.; Yang, Y. L.; Zeng, Q. D.; Wang, C. *J. Phys. Chem. C* **2007**, *111* (26), 9235–9239.
(29) Li, C. J.; Zeng, Q. D.; Liu, Y. H.; Wan, L. J.; Wang, C.; Wang, C. R.; Bai, C. L. *ChemPhysChem* **2003**, *4* (8), 857–859.
(30) Yamada, R.; Wano, H.; Uosaki, K. *Langmuir* **2000**, *16* (13), 5523–5525.
(31) Ruben, M.; Payer, D.; Landa, A.; Comisso, A.; Gattinoni, C.; Lin, N.; Collin, J. P.; Sauvage, J. P.; De Vita, A.; Kern, K. *J. Am. Chem. Soc.* **2006**, *128* (49), 15644–15651.
(32) Lackinger, M.; Griessl, S.; Heckl, W. M.; Hietschold, M.; Flynn, G. W. *Langmuir* **2005**, *21* (11), 4984–4988.

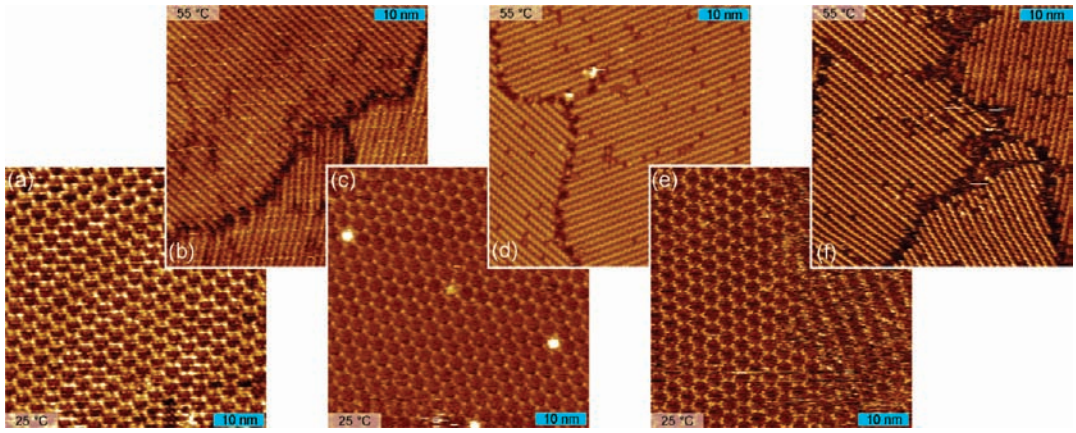

Figure 2. STM topographs as acquired during repeated heat−cool cycles of saturated BTB in nonanoic acid solutions demonstrating the reversibility of the phase transition. The respective temperature is stated in the lower (upper) left corner of each image. The cycle starts at the lower left image (a) at room temperature (V_{bias} = 1.15 V, I_T = 71 pA) and is continued (b) at 55 °C (V_{bias} = 1.15 V, I_T = 72 pA) → (c) at 25 °C (V_{bias} = 1.15 V, I_T = 65 pA) → (d) at 55 °C (V_{bias} = 1.15 V, I_T = 73 pA) → (e) at 25 °C (V_{bias} = 1.15 V, I_T = 77 pA) → (f) at 55 °C (V_{bias} = 1.15 V, I_T = 79 pA).

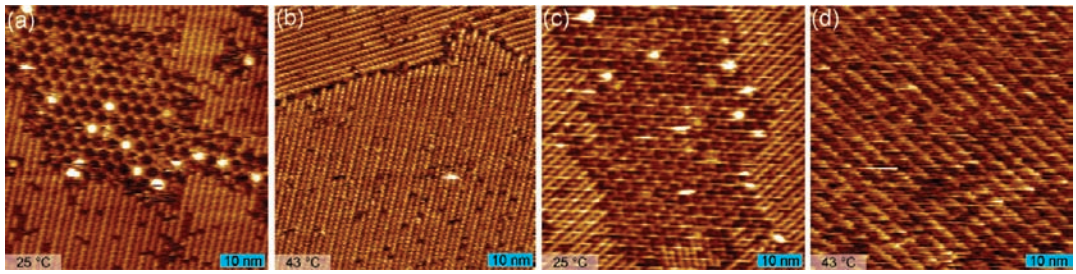

Figure 3. STM topographs as obtained from repeated heat−cool cycles of saturated BTB in octanoic acid solutions demonstrating the reversibility of the phase transition. The respective temperature is stated in the lower left corner of each image. The series starts at the left image (a) at room temperature (V_{bias} = 1.10 V, I_T = 92 pA) and is continued (b) at 43 °C (V_{bias} = 1.10 V, I_T = 78 pA) → (c) at 25 °C (V_{bias} = 1.10 V, I_T = 56 pA) → (d) at 43 °C (V_{bias} = 1.10 V, I_T = 85 pA).

(cf. Figures 2 and 3). In both solvents, the chicken-wire structure reappears below the temperature thresholds of ∼43 °C (**8A**) and ∼55 °C (**9A**), respectively. In some cases in **9A** small patches of the row structure emerged after the first cycle.

Concentration Dependence. While all studies described above were conducted with saturated solutions, further experiments were carried out with diluted solutions. Solubilities of BTB are 0.77 mM in **7A**, 0.75 mM in **8A**, and 0.50 mM in **9A**; thus all saturated solutions exhibit comparable concentrations. At BTB concentrations in **7A** of about 50% saturation, the row structure assembled on the surface coexisting with the chicken-wire structure. For more diluted solutions, at concentrations around 10% saturation, the chicken-wire structure is the dominating polymorph, emphasizing the importance of solute concentration in molecular self-assembly. Concentration-induced polymorphism, where the less densely packed polymorphs emerge for more diluted solutions, was found for various other systems.[18,19,33] As concluded from thermodynamic considerations, the observation of coexistence of both polymorphs over a wide concentration range can be taken as an indication that their free energies are very similar.[19] As a singular experiment we explored possible phase transitions in 50% saturated solution of BTB in **9A**. However, at temperatures up to ∼70 °C no phase transition was observable, therefore pointing toward a relation between concentration and transition temperature.

Discussion

With respect to the adsorption geometry of BTB molecules and adsorbate−substrate and intermolecular interactions, the row and chicken-wire polymorphs are entirely different. In the chicken-wire structure BTB molecules adsorb planar on the surface and are interconnected by linear double O−H···O hydrogen bonds between carboxylic groups, as thoroughly discussed elsewhere.[15] The hexagonal unit cell (a = 3.2 nm) contains two molecules. Likewise, the unit cell of the row structure (unit cell parameters: a = 3.3 nm, b = 0.7 nm, 82° angle) contains two molecules, but its relatively small area readily indicates nonplanar adsorption. The row structure is also comparable to the monolayer morphology found for a slightly larger tricarboxylic acid,[14] in which molecules are stacked face-to-face along columns parallel to the substrate. The monolayer is then comprised of densely packed parallel rows. In the row structure molecules adsorb nearly upright; thus the molecule−substrate interaction is diminished as compared to planar adsorption. However, intermolecular van der Waals and $\pi-\pi$ interactions stabilize the structure. BTB molecules adsorb with two carboxylic groups on the substrate, while the third carboxylic group points off the surface into the solution. According to our structural model, inter-row O−H···O hydrogen bonds are feasible, yet their unfavorable geometry and the absence of resonance effects that stabilize cyclic hydrogen bonds render

(33) Meier, C.; Roos, M.; Künzel, D.; Breitruck, A.; Hoster, H. E.; Landfester, K.; Gross, A.; Behm, R. J.; Ziener, U. *J. Phys. Chem. C* **2010**, *114* (2), 1268–1277.

Table 1. Comparison of Packing Density, Enthalpic Gain (Δh_{eff}), Entropic Cost ($-T\Delta s$), and Free Energy of Adsorption (Δg) per Unit Area of the Two Polymorphs at Two Reference Temperatures of 300 and 350 K[a]

	packing density (10^{14} cm^{-2})	Δh_{eff} (μJ cm^{-2})	$-T\Delta s$(@300 K) (μJ cm^{-2})	$-T\Delta s$(@350 K) (μJ cm^{-2})	$\Delta g = \Delta h_{eff} - T\Delta s$(@300 K) ($\mu$J cm^{-2})	$\Delta g = \Delta h_{eff} - T\Delta s$(@350 K) ($\mu$J cm^{-2})
chicken-wire (without solvent coadsorption)	0.23	−5.8	+3.9	+4.6	−1.9	−1.2
chicken-wire (with 8 × **9A** solvent molecules coadsorbed)	0.23 (BTB) 0.90 (**9A**)	−23.7	+14.6	+17.1	−9.1	−6.6
row	0.87	−18.5	+14.8	+17.3	−3.7	−1.2

[a] Stabilizing enthalpic contributions are assumed to be temperature independent. Δh_{eff} refers to values derived from molecular mechanics calculations; Δs is calculated using eqs 1 and 2.

them energetically inferior as compared to the double hydrogen bonds of the chicken-wire structure. Based on STM-derived unit cell parameters, the packing densities of the polymorphs amount to 0.23 molecules nm^{-2} for the chicken-wire and 0.87 molecules nm^{-2} for the row structure, respectively.

Thermodynamics. In the following we discuss whether the experimentally observed structure always represents the thermodynamically most stable polymorph at the respective temperature, i.e., the polymorph that yields the lowest Gibbs free energy. For monolayer self-assembly at the liquid−solid interface the whole system including the solution needs to be considered to evaluate all thermodynamic contributions. From an entropic point of view, adsorption and self-assembly of molecules from solution is unfavorable because molecules lose degrees of freedom and thus entropy upon aggregation. On the other hand, favorable enthalpic contributions arise from attractive molecule−substrate and molecule−molecule interactions. A balance of both contributions (entropy and enthalpy) steers self-assembly, and renders it a thermodynamically driven process. In order to gain insight into the thermodynamic properties of the two BTB polymorphs, the various entropic contributions were partitioned and estimated according to a method proposed by Whitesides and co-workers and similarly employed by Krissinel and Henrick.[34,35] When molecules assemble into supramolecular complexes, the entropic penalty mainly arises from losses in translational, rotational, conformational, and vibrational entropy, $\Delta S_{tot} = \Delta S_{trans} + \Delta S_{rot} + \Delta S_{conf} + \Delta S_{vib}$. Since BTB molecules do not possess significant internal degrees of freedom, conformational entropy losses can be neglected. Because of their relatively high energy in comparison to thermal energy, intramolecular vibrations do not significantly contribute to the entropy and can also be neglected.[34] The following equations provide reasonable estimates for the two relevant entropy terms for soluted molecules:

$$S_{trans} = R \ln[c^{-1}(2\pi m k_B T e^{5/3}/h^2)^{3/2}] \quad (1)$$

$$S_{rot} = R \ln[\pi^{1/2}/\gamma(8\pi^2 k_B T e/h^2)^{3/2}(I_1 I_2 I_3)^{1/2}] \quad (2)$$

Here, h is Planck's constant, k_B the Boltzmann constant, R the gas constant, and T the absolute Temperature, while e is Euler's number, m is the solute's mass, and c is the solute concentration. Furthermore, γ considers the symmetry of the molecule, and I_1, I_2, and I_3 are its principle moments of inertia. In order to avoid overestimation of translational entropy, concentrations are related to the free volume of the solvent as proposed by Whitesides and co-workers. The free volume of a solvent can be estimated by the hard cube approximation[34] and is significantly smaller than the actual volume, e.g., ∼32 mL for 1 L of heptanoic acid. It is assumed that upon adsorption molecules entirely lose their translational and rotational entropy, consequently eqs 1 and 2 allow estimating the entropic loss for adsorption of a single BTB molecule from solution. In the same manner, the entropic losses for coadsorbed solvent molecules can be estimated.

In order to compare the entropic costs for the two polymorphs, contributions from rotational and translational entropy were calculated assuming saturated solutions. For all three solvents, the entropic cost for BTB adsorption has a similar value of −0.190 kJ mol^{-1} K^{-1} for translational and −0.152 kJ mol^{-1} K^{-1} for rotational entropy. In order to estimate the entropic cost per unit area for self-assembly of a pure monolayer of the respective polymorph, the total entropy loss of −0.342 kJ mol^{-1} K^{-1} was then combined with STM-derived molecular packing densities. Numbers for the entropic contribution to the free energy at 300 K (room temperature) and 350 K respectively are provided in Table 1. It can be clearly seen that the row structure is entropically far less favorable than the chicken-wire structure, due to its 3.8-fold higher packing density. The entropic cost becomes even more pronounced at elevated temperatures. However, the situation is altered when solvent coadsorption within the cavities of the chicken-wire structure is taken into account. Although coadsorbed solvent molecules have not been directly observed in this study, probably due to their low stabilization energy and short residence times, coadsorption of guest molecules within open-pore networks was observed experimentally[14,16,18,21] and has been recognized as an important stabilizing contribution.[12,13,19,33,36] For instance, coadsorption of coronene as molecular guest in the cavities of an open-pore dehydrobenzoannulene polymorph stabilizes this host−guest network thermodynamically in comparison to the densely packed polymorph.[36]

In the present case, up to eight solvent molecules (**8A** or **9A**) can be coadsorbed in each cavity of the chicken-wire structure

(34) Mammen, M.; Shakhnovich, E. I.; Deutch, J. M.; Whitesides, G. M. *J. Org. Chem.* **1998**, *63* (12), 3821–3830.
(35) Krissinel, E.; Henrick, K. *J. Mol. Biol.* **2007**, *372* (3), 774–797.
(36) Furukawa, S.; Tahara, K.; De Schryver, F. C.; Van der Auweraer, M.; Tobe, Y.; De Feyter, S. *Angew. Chem., Int. Ed.* **2007**, *46* (16), 2831–2834.

(cf. Supporting Information Figure S4). Coadsorbed **9A** solvent molecules cause a translational entropy loss of -0.102 kJ mol^{-1} K^{-1} and a rotational entropy loss of -0.132 kJ mol^{-1} K^{-1}. Comparison of these values with the entropic losses for BTB adsorption points out that the total entropic cost increases more steeply with the number of adsorbed molecules rather than with the size and molecular weight of adsorbates. Since solvent coadsorption drastically increases the number of adsorbed molecules, the associated entropic cost of the chicken-wire structure becomes significantly enhanced. The relatively large entropic contributions to Gibbs free energy of both solute and solvent molecules (cf. Table 1) underline the fact that entropy considerations have to be taken into account for thermodynamics of monolayer self-assembly.

A quantitative comparison of the stabilizing enthalpic contributions between the two polymorphs is more difficult because different types of interactions (i.e., hydrogen bonds vs van der Waals and $\pi-\pi$ interactions) need to be compared. Molecular mechanics (MM) simulations are well suited to evaluate the energetics of van der Waals interactions. However, standard force fields seriously underestimate the strength of cyclic resonance stabilized hydrogen bonds.[37] In order to make a valid comparison of binding enthalpies, MM results using the Dreiding force field for the chicken-wire polymorph are combined with the experimentally and theoretically well-established binding enthalpy of -60 kJ mol^{-1} for the 2-fold O$-$H$\cdots$O hydrogen bond between two carboxylic groups.[38]

According to the proposed method, the average binding enthalpy of BTB molecules in the chicken-wire structure amounts to -332 kJ mol^{-1}. This value originates from the combination of a MM-derived molecule$-$substrate interaction of -242 kJ mol^{-1} with the binding enthalpy due to intermolecular hydrogen bonds of -90 kJ mol$^{-1} = 3 \times 0.5 \times -60$ kJ mol^{-1}. In the chicken-wire structure all three carboxylic groups of each molecule form 2-fold intermolecular hydrogen bonds, while the factor 0.5 corrects for overcounting of pairwise interactions.

The row structure is predominantly stabilized by van der Waals interactions, and the average binding enthalpy was evaluated by MM computations, which yield a value of -308 kJ mol^{-1} (cf. Supporting Information for details). As anticipated, the adsorbate$-$substrate binding is inferior in the row structure (-176 kJ mol^{-1}), but due to the high packing density and mutual molecular arrangement the intermolecular van der Waals and $\pi-\pi$ interactions are superior.

Last, the stabilizing effect of coadsorbed solvent molecules within the cavities of the chicken-wire structure is calculated. Coadsorption of eight **9A** solvent molecules in one cavity of the chicken-wire structure yields an enthalpic contribution of -940 kJ mol^{-1} per unit cell (cf. Supporting Information for a structural model and details of the calculation).

Binding enthalpies obtained from the above methods refer to isolated, geometry-optimized molecules under vacuum. Yet, the appropriate reference state for these considerations is dissolved and solvated solute molecules.[39] Solvation enthalpies lower the effective binding enthalpies significantly. In comparison to experiments under ultra-high-vacuum conditions, desorption barriers are substantially lower at the solid$-$liquid interface, which gives rise to an effective adsorption$-$desorption equilibrium even for comparatively large compounds.[13,18,36] Corrections of the adsorption enthalpy due to solvation were included by assuming that the interaction of dissolved solute molecules in solution is governed by intermolecular solvent$-$solute or solute$-$solute hydrogen bonds, where each of the three carboxylic groups of BTB forms a 2-fold hydrogen bond with a binding enthalpy of -60 kJ mol^{-1}. Consequently, solvation lowers the effective binding enthalpy of each molecule by at least $+180$ kJ mol^{-1}.

On the basis of the estimates of both entropic cost and enthalpic gain, the free energies of adsorption of each polymorph were evaluated for two reference temperatures. Since in all experiments the surface coverage is close to unity, we will refer to Gibbs free energy of adsorption per unit area A: $\Delta g = \Delta G/A = \Delta H/A - T\Delta S/A = \Delta h - T\Delta s$ (note that Δh and Δs, i.e., enthalpy and entropy changes per unit area upon monolayer self-assembly, are both negative). The results are summarized in Table 1. For the chicken-wire polymorph two scenarios were considered, with and without coadsorption of solvent (**9A**).

For room temperature the figures in Table 1 indicate that the row structure is thermodynamically favored over the pure chicken-wire polymorph, i.e., when solvent coadsorption is neglected. However, despite its large entropic cost, solvent coadsorption still stabilizes the chicken-wire polymorph at room temperature and even renders this bimolecular monolayer the thermodynamically most stable polymorph in **9A**. At elevated temperature, the free energy gain associated with self-assembly of a monolayer row structure becomes comparable to the chicken-wire structure without coadsorbed solvent due to the increased entropic cost of the more densely packed polymorph. On the basis of these estimates of Δg, the following explanation for the reversible phase transition is proposed: With the aid of solvent coadsorption, the chicken-wire polymorph is the thermodynamically most stable polymorph at room temperature in **9A**. Upon increasing the temperature, coadsorbed solvent molecules start to desorb first, while the chicken-wire network is still stable. Coadsorbed solvent molecules are less tightly bound than BTB molecules, as the latter—due to their size—have increased interaction with the substrate and are additionally stabilized by six hydrogen bonds. Once the chicken-wire structure lacks the stabilizing contribution from solvent coadsorption, the free energy of adsorption of the row structure becomes comparable, giving rise to the phase transition. The proposed model also consistently explains the solvent dependence of the transition temperature. The binding enthalpies of fatty acid molecules on graphite increase approximately linearly with their aliphatic chain length. Accordingly, the desorption temperature of **8A** solvent molecules is lower than that of **9A** molecules. In the thermodynamic competition between chicken-wire and row structure, easier desorption leads to a lower transition temperature in **8A** than in **9A** solutions or a transition temperature even below room temperature as observed for **7A**.

Although in the present case a molecule-based evaluation of thermodynamic quantities yields the correct trends, a word of caution is appropriate. The Gibbs free energies of adsorption and the relative thermodynamical stabilities of these polymorphs sensitively depend on the subtle balance of adsorbate$-$adsorbate, adsorbate$-$substrate, and solute$-$solvent interactions. A quantitative thermodynamic discussion of the complex situation of monolayer self-assembly at the liquid$-$solid interface is challenging primarily because of inaccuracies in the evaluation of

(37) Martsinovich, N.; Troisi, A. *J. Phys. Chem. C* **2010**, *114* (10), 4376–4388.
(38) Neuheuser, T.; Hess, B. A.; Reutel, C.; Weber, E. *J. Phys. Chem.* **1994**, *98* (26), 6459–6467.
(39) Meier, C.; Landfester, K.; Künzel, D.; Markert, T.; Gross, A.; Ziener, U. *Angew. Chem., Int. Ed.* **2008**, *47* (20), 3821–3825.

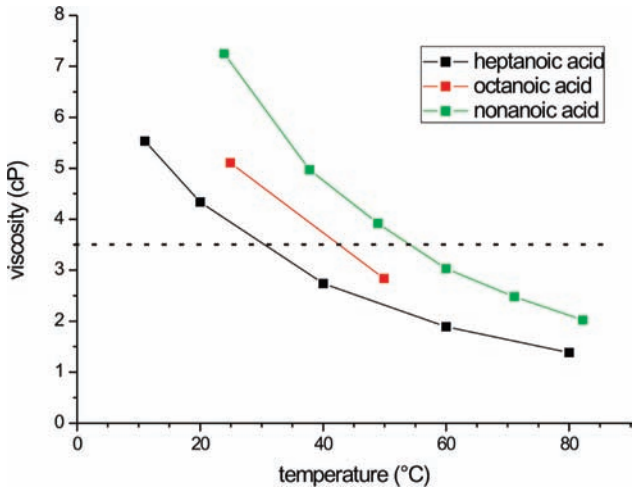

Figure 4. Viscosities of pure heptanoic (**7A**), octanoic (**8A**), and nonanoic acid (**9A**) as a function of temperature,[41] depicting the inverse dependence of viscosity on temperature. The dashed line indicates a value of 3.5 cP.

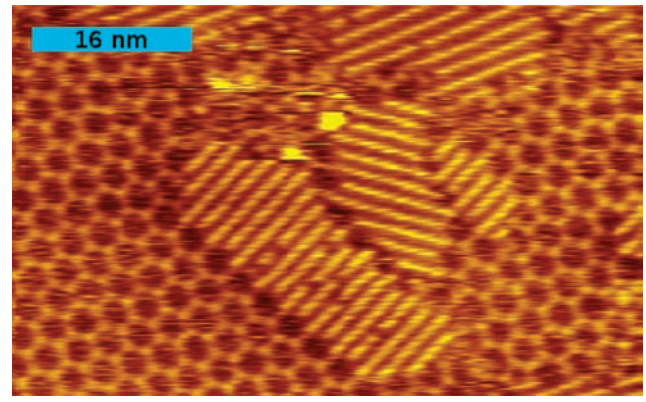

Figure 5. STM topograph of a BTB monolayer in nonanoic acid (**9A**) after heating and cooling. Patches of the row structure are observable and coexist with the chicken-wire structure. The lower left phase boundary exemplifies a general observation: the rows are aligned with the chicken-wire structure. Every other row is connected to molecules from the chicken-wire polymorph; rows in between end in cavities.

both entropic and enthalpic contributions, but also due to hardly assessable contributions, as for instance from solvation. Also, for solvent coadsorption precise structural data are not available.

Nevertheless, established methods to estimate entropic costs and evaluation of binding energies based on molecular mechanics and experimental values for hydrogen bond energies allow at least a semiquantitative evaluation of Gibbs free energies of adsorption of competing monolayer polymorphs. Although the exact prediction of crossing points as a function of concentration or temperature is hardly possible, at least a qualitative understanding of trends can be obtained. On the other hand, kinetic effects might also play an important role for monolayer self-assembly. From basic considerations, we conclude that the adsorption rate of solute molecules is proportional to c/η, where c stands for the solute concentration and η for the solvent viscosity (cf. Supporting Information). Interestingly, the viscosities of all three solvents in this study are considerably different at room temperature and crucially depend on temperature as depicted in Figure 4. Also, the viscosities of **7A**, **8A**, and **9A**, and thus the adsorption rate, correlate inversely with temperature and vary appreciably within the relevant temperature interval.

Further interesting aspects are topological and epitaxial similarities between chicken-wire and row structure: As illustrated in Figure 5, STM topographs of both coexisting polymorphs clearly show a structurally well-defined heterointerface. Moreover, the direction of the rows is aligned with the cavities of the chicken-wire polymorph. Both facts indicate that a morphological transition from chicken-wire to row polymorph might be initiated by filling of empty cavities of the chicken-wire structure with excess BTB molecules. Under conditions where the row structure becomes thermodynamically favored, this phase transition can also be understood as a cross nucleation event, i.e., a special case of heterogeneous nucleation where a thermodynamically more stable polymorph nucleates on a preexistent metastable modification.[40]

De Feyter et al. discussed and modeled the concentration dependence of bimorphic monolayer self-assembly in detail.[19] Similarly, by means of a slightly different model, Meier et al. conclude that densely packed polymorphs become thermodynamically preferred at higher solute concentrations.[33] In both cases, at low concentrations, an open-pore structure is favored over a densely packed structure, just as in the present case for BTB in **7A**. The thermodynamic model proposed by de Feyter et al. also includes a temperature-dependent term, which results in a diminished coverage ratio of open-pore to densely packed polymorph at elevated temperatures. Consequently, their model seems generally applicable and can also explain the temperature-dependent phase transition, provided that the chemical potential of BTB molecules in the row structure is sufficiently large.

Conclusions and Outlook

By means of STM reversible temperature-driven phase transitions have been observed for BTB monolayers at the liquid−solid interface. Carboxylic acids were used as solvents, and transition temperatures were found to depend on type of solvent and concentration. The two polymorphs differ significantly in packing density, arrangement of molecules, and intermolecular interactions. Both morphologies are known, and analogues have previously been reported for other tricarboxylic acids.[14,15] Estimates of the entropic cost and enthalpic gain upon monolayer self-assembly of both polymorphs suggest that a thermodynamic explanation for the phase transition in view of Gibbs free energy of adsorption is only appropriate when solvent coadsorption is taken into account. Solvent coadsorption within the cavity voids of the nanoporous chicken-wire structure has a high entropic cost because the number of adsorbed molecules is large. However, this entropic cost is still outweighed by the associated enthalpic gain. In order to explain the phase transition, we propose that desorption of coadsorbed solvent molecules

(40) Yu, L. *CrystEngComm* **2007**, *9* (10), 847–851.

(41) Landolt-Börnstein *Tabellenwerk Zahlenwerte und Funktionen aus Physik, Chemie, Astronomie, Geophysik und Technik*; Springer: Berlin, **2002**; Vol. 18 B.

eventually destabilizes the chicken-wire polymorph and leads to the emergence of the row structure. This purely thermodynamic model inherently explains the reversibility of the phase transition. However, the kinetics of adsorption and desorption can also determine the experimental observations. For instance, the row structure patches that were occasionally observed in **9A** after the first heat−cool cycle might be attributed to a slow desorption kinetics of BTB molecules in the row structure. Mostly because of the strong temperature dependence of solvent viscosity, also the adsorption kinetics changes significantly with temperature.

There is one particularly intriguing aspect to the phase transition from chicken-wire to row structure: it closes supramolecular cavities. This effect may be utilized for the controlled release of molecular guests with conceivable medical and life-science applications. With this in mind, it would be highly interesting to explore whether adsorption of deliberate molecular guests other than coadsorbed solvent molecules within the pores of the chicken-wire structure hampers the phase transition, thus leading to increased transition temperatures or even suppression of the phase transition.

Acknowledgment. Financial support by the Deutsche Forschungsgemeinschaft (Sonderforschungsbereich 486, FOR 516), the Bayerische Forschungsstiftung, and the Nanosystems Initiative Munich (NIM) is gratefully acknowledged.

Supporting Information Available: Experimental details, kinetic considerations, additional STM topographs, and details of molecular mechanics simulations. This material is available free of charge via the Internet at http://pubs.acs.org.

JA908919R